ERJ Express. Published on July 16, 2009 as doi: 10.1183/09031936.00181808

Bleomycin induces pleural and subpleural fibrosis in the presence of carbon particles

Decologne N[*•], Wettstein G[*•], Kolb M[†], Margetts P[†], Garrido C[*], Camus P[*,‡], Bonniaud P[*,‡]

[*] Institut National de la Santé et de la Recherche Médicale (INSERM) UMR 866, University of Burgundy, 7 bd Jeanne d'Arc, 21000 Dijon, France

[†] Centre for Gene Therapeutics, Department of Pathology and Molecular Medicine, McMaster University, 1200 Main St W, Hamilton, ON, Canada L8N 3Z5

[‡] Service de Pneumologie et Réanimation Respiratoire CHU du Bocage, 21079 Dijon, France, www.pneumotox.com

[•] These authors have contributed equally to this work.

Corresponding author:

Philippe Bonniaud, MD, PhD

Service de Pneumologie et Réanimation Respiratoire, CHU du Bocage

21079 Dijon, France

Tel : (+33) 3 80 29 32 48

Fax (+33) 3 80 29 36 25

Email: philippe.bonniaud@chu-dijon.fr

Funding, Financial support: The research leading to these results has received funding from the European Community's Seventh Framework Programme (FP7/2007-2013) under grant agreement n° HEALTH-F2-2007-202224 eurIPFnet.. N.D. is supported by the "Société de Pneumologie de Langue Française" the "Ligue Bourguignonne contre le cancer", and the "Association pour la Recherche sur le Cancer". G.W. is supported by the EU 7th Framework 2007-2013 n° HEALTH-F2-2007-202224 eurIPFnet. M.K. has a New Investigator Award from CIHR. C.G. is supported by grants from the "Ligue Nationale Contre le Cancer" and its committees in the "Nièvre" and "Saône-et-Loire".

Running title: Bleomycin induces pleural and subpleural fibrosis

Word count for the text: 3718

Word count for the abstract: 200

Number of figures: 6

Number of tables: 2

Abstract

The pathologic changes in idiopathic pulmonary fibrosis typically start within subpleural lung regions, a feature that is currently not explained. IPF as well as bleomycin-induced lung fibrosis are more common in smokers. We hypothesized that carbon particles, major components of cigarette smoke that are transported to alveoli and pleural surface, might be involved in the development of subpleural fibrosis through interaction with pleural mesothelial cells.

Carbon particles were administered to mice in combination with bleomycin through intratracheal and/or intrapleural injection and fibrosis was assessed using histomorphometry.

Carbon administered to the chest cavity caused severe pleural fibrosis in the presence of bleomycin, whereas bleomycin alone had no fibrogenic effect. The pleural response was associated with progressive fibrosis in subpleural regions, similar to human IPF. Matrix accumulation within this area evolved through "mesothelial-fibroblastoid transformation" where mesothelial cells acquire myofibroblast characteristics. In contrast, carbon did not exaggerate bleomycin-induced pulmonary fibrosis after combined intratracheal administration.

Conclusion: This represents a novel approach to induce a robust experimental model of pleural fibrosis. It also suggests that carbon particles might be involved as a co-factor in the initiation and/or progression of (subpleural) pulmonary and pleural fibrosis. Mesothelial cells appear to be critical contributors to this fibrotic process.

Key words: drug-induced pneumonitis; epithelial to mesenchymal transition; idiopathic pulmonary fibrosis; myofibroblast; pleura; transforming growth factor - beta

INTRODUCTION

Fibrosis is a common denominator of chronic disorders, including lung diseases such as asthma, pulmonary fibrosis, pulmonary hypertension and pleural fibrosis. Pleural and pulmonary fibrosis have many features in common. The obvious are that both disorders are characterized by excessive deposition of extracellular matrix (ECM) and result in a restrictive impairment of lung function. Pleural fibrosis as a disease entity is less recognized as pulmonary fibrosis, but it nevertheless can cause severe functional impairment and markedly reduce quality of life. The initiating events for pleural fibrosis are often identifiable, and include drugs, radiation, asbestos, haemothorax, thoracotomy for coronary bypass and - most often - infectious diseases [1]. This is in strong contrast to Idiopathic Pulmonary Fibrosis (IPF), where per definition no underlying cause is found. However, there are cases in which even pleural fibrosis is idiopathic, and they are typically progressive and lead to death [2-4]. Similar to IPF, there is no effective therapy to reverse established pleural fibrosis. Conversely to its negative impact as disease, pleural fibrosis can become a desirable therapeutic approach in order to treat the accumulation of refractory pleural effusion. Thus, research of mechanisms of pleural fibrosis and of effective pleurodesing agents is highly relevant and has excitingly divergent angles [5, 6].

IPF usually progresses quite rapidly over years and always compromises pulmonary function. The disease is characterized by myofibroblast proliferation and accumulation of fibroblastic foci, which along with progressive collagen deposition destroy the lung architecture. Recent evidence suggests that IPF is the result of abnormal healing responses to repeated microscopic injury of the lung. Interestingly, one of the hallmarks of IPF is that not only early abnormalities but also advanced fibrosis is predominantly located in the subpleural regions [7]. This characteristic and to date unexplained feature of IPF was one of the

rationales for the experiments described in our study, besides the investigation of pleural fibrosis itself. We recently reported that overexpression of the fibrogenic cytokine transforming growth factor (TGF)-β1 in the pleural space does not only induce progressive pleural fibrosis, but is also associated with abnormal collagen deposition within the subpleural lung parenchyma. We also demonstrated that mesothelial cells play a critical role in pleural fibrosis and we proposed that they may be involved in the subpleural initiation of IPF [8].

Bleomycin is well known to induce a toxic response leading to lung fibrosis in humans [9, 10]. Bleomycin is also an efficient and the most widely used compound for induction of experimental pulmonary fibrosis in animals. In contrast, it is rather difficult to generate pleural fibrosis in small rodents using bleomycin, although it is a valid option for therapeutic pleurodesis in humans [11]. Cigarette smoke is a risk factor for the development of IPF [12] and bleomycin-induced lung fibrosis in patients [13], and it can exaggerate experimental fibrosis in rodents [14]. It is unclear, if a specific compound in cigarettes enhances the fibrogenic process or if this is due to the additional alveolar injury. Tobacco smoke is a complex mixture of more than 4000 chemicals, and - like other by-products of combustion - contains considerable numbers of ultrafine particles [15]. Carbon particles are found in cigarette smoke and in pollution, while carbon black is also widely used in the industry. Once inhaled, these particles can reach the alveolar lumen and move towards the pleural surface [16]. It is very likely that the microscopic alveolar injury proposed to exist in IPF is caused by several noxious insults, and we hypothesized that cigarette smoke components, specifically carbon particles might be involved as one of the co-factors in the initiation and/or progression of (subpleural) pulmonary and pleural fibrosis.

In the present work we examined the effect of carbon on bleomycin-induced fibrotic disease of the pleura and lung. We found that carbon particles did not worsen bleomycin-

induced fibrosis in lung tissue, but were critical for the induction of pleural and subpleural fibrosis after intrapleural administration of bleomycin. We provide evidence suggesting that mesothelial cells play an important role in this process.

METHODS

Animal Procedures

Female Swiss CD1 mice (Charles River, Saint Germain-sur-l'Arbresle, France) were housed in pathogen-free conditions. Rodent food and water were provided *ad libitum*. The animals were treated according to the guidelines of the "Ministère de la Recherche et de la Technologie", France. All experiment were approved by "Comité d'Ethique de l'Université de Bourgogne". Procedures were performed with inhalation anaesthesia with isoflurane (TEM, Lormont, France). *For* ***intratracheal instillation***, animals received 50 µl NaCl 0.9%, carbon (carbon black 101, 90 nm diameter, Degussa, Frankfurt, Germany) 0.1 mg/mouse, bleomycin (blenoxane, Bristol Laboratories Canada) 0.07 U/mouse or bleomycin + carbon *via* a 22G canula introduced within the trachea without surgery. Bleomycin and carbon were diluted in NaCl 0.9%. For ***intrapleural administration,*** animals received an intrapleural injection (100 µl) as previously described [8], of NaCl 0.9%, carbon (0.1 mg/mouse), bleomycin (0.07 U/mouse or 0.48 U/mouse) or bleomycin + carbon.

Pleural lavage fluid (PLF), bronchoalveolar lavage fluid (BALF) and lungs were harvested as previously described [8]. Briefly, after abdominal aortic bleeding and slight incision through the diaphragm, PLF was performed with 1.2 ml of NaCl 0.9% injected into the pleural space. A canula was placed into the trachea, lungs were removed and BAL was performed with 1 ml of NaCl 0.9%. Lungs were inflated with and placed in formalin for 24 hours. PLF and BALF were centrifuged and supernatants were stored at -80°C. Cytospins of pellets were counted (Giemsa).

Pleurodesis score

The macroscopic pleurodesis was graded [17]: 0 – normal pleura; 1 – < three adhesions; 2 – > three adhesions, but localised; 3 – generalised scattered adhesions; 4 – complete obliteration of pleural space.

TGF-β1 levels

Total human TGF-β1 was determined from PLF or culture supernatant using ELISA (R&D Systems, Lille, France), performed according to the recommendations of the manufacturer. The sensitivity of this assay is 7 pg/ml.

Histology

Transverse sections were paraffin-embedded, 5-µm-sectioned, and stained with Masson-Trichrome and Picrosirius Red. HSP47 immunohistochemistry and dual staining immunofluorescence with antibodies to α-smooth muscle actin (α-SMA) and cytokeratin were performed as previously described [8]

The pleura thickness was determined by histomorphometric measurement on sections stained with Masson-Trichrome (200X) as previously described [8]: twenty random measures per section per animal (Eclipse E600 microscope, Nikon, Champigny-sur-Marne, France). Pictures (colour camera 3 CCD, Sony, Nikon, Champigny-sur-Marne, France) were analysed using an analyzing system (Archimed Instruments, Evry, France).

Collagen was analyzed on sections stained with Picrosirius Red (200X) as previously described [8]: twenty random fields per animal were digitized under polarized light. The percentage of emission was quantified (morphometry software Histolab, Microvision Instruments, Evry, France) as a reflection of collagen content. Collagen intensity in the pleura was measured within a rectangle (constant length of 100 µm, width depending on pleura

thickness). Collagen content was expressed as % emission multiplied by the surface of each rectangle. Collagen within the subpleural zone was measured using circles (diameter 65 μm) randomly placed at constant distance from the pleural surface (Fig 2D). Collagen content within circles was expressed as % emission.

Zymography

The gelatinolytic activity of MMP-2 and -9 in PLF or cell culture supernatants was measured by zymography [8]. Samples were separated by 10% sodium dodecylsulfate-polyacrylamide gel electrophoresis containing 0.1% gelatin (Sigma, St Quentin Fallavier, France). After electrophoresis, the gels were incubated in 2.5% Triton X-100 (Sigma, St Quentin Fallavier, France) for 30 min and were then placed in the activating buffer (50 mM Tris-HCl pH 8, 10 mM $CaCl_2$, 5 μM $ZnSO_4$, 150 mM NaCl, Sigma, St Quentin Fallavier, France), overnight at 37°C. The gels were stained with 0.1% Coomassie brilliant blue-250 solution (Sigma, St Quentin Fallavier, France), during 30 min at 37°C. The gels were then destained with several changes of 40% methanol and 7% acetic acid. Zones of enzymatic activity were evident as clear bands against blue background. Reference standards were MMP-2 and -9 (Chemicon International, Paris, France).

Mesothelial cell culture

Primary culture of mesothelial cells was performed from female Sprague Dawley rats (Charles River, Saint Germain-sur-l'Arbresle, France). Rats were euthanized by abdominal aortic bleeding. After incision through the diaphragm, 10 ml trypsin-0.4% EDTA was injected in the pleural cavity. After 30 minutes, the fluid was aspirated and put into 15 ml Fetal Calf Serum (FCS), centrifuged at 1,300 rpm for 5 minutes and the pellet was re-suspended in Dulbecco's Modified Eagle's Medium (DMEM) with 1% L-Glutamine, 1%

Penicillin-Streptomycin and 15% FCS. The cells were incubated at 37°C with 5% CO_2. To confirm the mesothelial cell phenotype, we performed immunofluorescence staining for calretinin (Santa Cruz, TebuBio, Le Peray en Yvelines, France). Briefly, cultured mesothelial cells fixed by 4% paraformaldehyde and made permeable by Triton X-100, were incubated with calretinin (1/100) overnight and then with secondary antibody (1/2000, biotinylated goat anti-mouse/rabbit Ig, Dakocytomation, Trappes, France).

4/4RM4 mesothelial cells were incubated in Ham's F10 with 1% L-Glutamine, 1% Penicillin-Streptomycin and 15% FCS. The cells were incubated at 37°C with 5% CO_2.

Mesothelial cells (primary and 4/4RM4) were cultured, without FCS, with carbon (250 µg/ml), bleomycin (25 mU/ml) or bleomycin + carbon for 48h. Carbon was suspended in medium by ultrasound.

Immunofluorescence

Staining with antibodies to E-cadherin (BD System, Le Pont-de-Claix, France) and α-smooth muscle actin (α-SMA, DakoCytomation, Trappes, France) was performed using fluorescently labelled antibodies. Briefly, 4/4RM4 mesothelial cells (ECACC, Rat Fisher visceral pleura mesothelium) were fixed by 4% para-formaldehyde and made permeable by Triton X-100, incubated with primary antibody (1/100) overnight and then with secondary antibody (1/2000,biotinylated goat anti-mouse/rabbit Ig, DakoCytomation, Trappes, France).

Statistical analysis

Comparisons between groups were performed by Mann Whitney test and comparisons between animals in the same group by Wilcoxon test.

RESULTS

Intratracheal administration of carbon black does not worsen bleomycin-induced pulmonary fibrosis.

Intratracheal NaCl or carbon did not induce inflammatory or fibrotic responses by day 21. As expected, intratracheal bleomycin caused pulmonary fibrosis by day 21 with persistent inflammation (Fig 1). Carbon co-administration did not alter bleomycin-induced inflammation or fibrosis. Collagen was significantly higher in both bleomycin groups, compared with saline and carbon, and was identical in bleomycin and bleomycin + carbon groups (Fig 1AB). Similar inflammation was observed in bleomycin and bleomycin + carbon groups (Fig 1A). Total cell count was similarly increased in BALF from bleomycin and bleomycin + carbon groups compared to saline and carbon ($p < 0.01$, not shown). There was no difference between groups in differential cell count.

Total TGF-β1 (Fig 1C) was significantly increased in BALF from bleomycin and bleomycin + carbon animals (96 +/- 41 and 109 +/- 55 pg/ml). Total TGF-β1 was not detectable in BALF from animals treated with NaCl or carbon.

Intrapleural co-administration of bleomycin and carbon induces severe and progressive pleural and subpleural fibrosis.

Mice receiving NaCl, carbon or bleomycin intrapleurally did not develop pleural fibrosis. There were some carbon spots on the pleural surface in carbon group by day 7, which disappeared by day 21 (Fig 2A). Microscopically, the pleura was a thin monolayer without collagen accumulation in NaCl and carbon groups. In the bleomycin group, there was a slight inflammatory response by day 7 (Fig 2B) that had resolved by day 21. Total cell number was similarly increased in PLF from carbon, bleomycin and bleomycin + carbon groups compared with NaCl. Neutrophils were increased in bleomycin and bleomycin + carbon groups (Table

1). Mice receiving bleomycin + carbon developed severe and progressive pleural fibrosis (Fig 2A). Pleural inflammation was apparent by day 7, progressively increased and fibrosis was a major feature by day 21 (Fig 2B). There were abundant adhesions, which complicated lung extraction; retrieval PLF was impossible. Histomorphometry showed increasing pleural thickness and collagen accumulation up to day 21 (Fig 2C). By day 21, the pleurodesis score (Table 2) after intrapleural injection of bleomycin + carbon was significantly higher (3.8 +/- 0.3) compared to the other groups (NaCl: 0 +/- 0, carbon: 0.3 +/- 0.3, bleomycin: 0.4 +/- 0.4).

Interestingly, the fibrotic changes in (bleomycin + carbon)-treated animals were not restricted to the pleura, but extended into the lung parenchyma adjacent to the pleural surface (Fig 2D). Collagen was quantified within this subpleural area by morphometry and progressive accumulation deep in the lung parenchyma was found (Fig 2D). Collagen was most prominent underneath the mesothelial cell layer (circle 1) and decreased with increasing distance from the surface (circle 2).

To our surprise, intraperitoneal or intranasal bleomycin concomitant with intrapleural carbon induced a strong fibrotic pleural response by day 21 (Fig 3), similar to combined intrapleural bleomycin + carbon administration.

In contrast to extracellular collagen, the collagen chaperon HSP47 [18] was induced in mesothelial cells in carbon, bleomycin and bleomycin + carbon by day 7, compared to NaCl. HSP47 was seen in the subpleural area only in (bleomycin + carbon)-treated mice along with collagen (Fig 4).

The tissue was analyzed for evidence “mesothelial-fibroblastoid transformation”, a process involving mesothelial cells and similar to epithelial to mesenchymal transition

(EMT)[8]. Zymography on PLF at day 7 showed increased MMP-9 activity in the bleomycin + carbon group (Fig 5A). The mesothelial layer from (bleomycin + carbon)-treated animals early on (day 7) contained a substantial number of cells positive for the epithelial marker cytokeratin and the myofibroblast marker α-SMA (dual staining immunofluorescence). By day 21, these dual-labelled cells persisted and numerous α-SMA-positive cells were present in the thickened pleura (Fig 5B), strongly suggesting transition of mesothelial cells to a myofibroblast phenotype. The bleomycin-treated mice had a smaller amount of dual-labelled cells within the pleura by day 7, which vanished by day 21 without evidence for increased persistence of α-SMA-positive cells. NaCl or carbon groups were normal at any time point. TGF-β1 is known to induce EMT and was significantly increased in PLF at day 7 in bleomycin and bleomycin + carbon groups (Fig 5C).

Mesothelial cells are active in this process

Primary rat mesothelial cells were exposed to carbon suspended in DMEM. After 48h, agglomerates of carbon were seen inside mesothelial cells, suggesting active ~~phagoyctosis~~ internalisation of these particles (Fig 6A). This was also observed in mesothelial cells in the animal model (Fig 6A). Gelatin-zymography on culture supernatants of mesothelial cells confirmed increased MMP-9 activity in both carbon groups (Fig 6B), similar to PLF.

4/4RM4 mesothelial cells exposed to bleomycin or to bleomycin + carbon showed, after 48h, an increase in α-SMA and a decrease in E-cadherin expression (Fig 6C).

DISCUSSION

The pleura is a biologically highly active structure. The mechanisms of pleural fibrosis are incompletely understood, and even more mysterious are the mechanisms of subpleural lung fibrosis, one of the hallmark of human IPF. Our work provides insight into the pathogenesis of both these fibrotic conditions and highlights a potential and to date unexplored role of the pleural mesothelium. The study also describes a novel rodent model of pleural fibrosis, which may have considerable impact on future research in the area of pleural fibrosis and pleurodesis.

The subpleural predominance of fibrosis is a characteristic feature of IPF, especially in the earlier disease stages [19]. There is no good explanation for this to date. Being aware of the relationship between smoking and IPF, we hypothesized that cigarette smoke could be involved not only in susceptibility to pulmonary and pleural fibrosis, but specifically in the development of the subpleural fibrosis pattern in IPF/UIP, possibly through carbon particles.

There are different models of lung fibrosis. All of them have certain advantages and limitations, depending on the underlying questions [20]. However, none of these experimental approaches truly models the subpleural fibrosis seen in human IPF [21]. Intratracheal injection of bleomycin is the most common method for induction of pulmonary fibrosis in animals. It consistently causes inflammation and fibrosis in rodent lungs, although the changes are limited and partially reversible [21]. Due to the mode of administration, fibrosis is predominantly peribronchial and central. Systemic bleomycin, e.g. delivered via osmotic mini-pumps or through repeated intraperitoneal injection, causes a more diffuse pattern of fibrosis in the lung, but again without the typical subpleural pathology of UIP [22]. In contrast to the parenchymal effect, bleomycin instilled in the pleural space rarely causes pleural fibrosis in rodents, although it can have some pleurodesis effects in humans [23].

Most research related to pleural scarring concerns the induction of pleurodesis as a therapeutic approach to treat chronic effusion associated with metastasized cancer. Rabbit or sheep models are typically employed for this purpose. Rodents, especially mice are preferred in experimental medicine, largely due to the availability of genetically manipulated strains that allow to dissect mechanistic questions in detail. In the context of experimental pleural fibrosis, there is a dramatic shortfall of rodent models, beside TGF-β overexpression with recombinant protein administration [24] or gene transfer [8]. Inflammation can be induced in mouse or rat pleura, but usually resolves over time, and chronic scarring and fibrosis rarely develops. The trigger for switching a resolving to a progressively fibrotic tissue response in the pleural cavity has not been identified yet. In this context, our new model should be of considerable interest.

Carbon particles are a component of cigarette smoke and a strong association between smoking and IPF/UIP has been shown before [12]. The role of cigarette smoke in pleural fibrosis is not as clear, but some studies have suggested a higher rate of asbestos related pleural fibrosis in smokers while others have not been able to confirm this [25]. Ultrafine or nanoparticles (size less than 100 nm) can enter the body through any exposed surface including lungs, skin, and the GI-tract [26]. Carbon black are nanoparticles believed to be inert and harmless to the lungs, although they can induce early and moderate, albeit transient inflammation [27]. There is a large database in the lung particle toxicology literature supporting significant toxic effects of a variety of nanoparticules [28]. Amongst all inhaled particles, asbestos fibers are probably best known for having the property to migrate from the parenchyma to the pleura [29]. This particle migration can occur through macrophage uptake or directly without involving cellular vehicles. Holt *et al*. demonstrated in guinea pigs that macrophages are able to carry carbon dust through the parenchyma towards the pleura [16]. In

our study, we administered carbon black together with bleomycin into the trachea or the pleural space of mice. We observed very severe pleural and subpleural fibrotic changes in mice receiving combined intrapleural bleomycin plus carbon, while neither bleomycin nor carbon alone caused fibrosis. As expected, intratracheal bleomycin resulted in inflammation and fibrosis, but this was not exaggerated by addition of carbon. This is similar to the work by Adamson *et al.* describing that carbon nanoparticles were retained in rodent lung when administered four days after bleomycin, but did not result in an increase of fibrosis [30]. Interestingly, we found that bleomycin does not need to be directly injected into the pleural space: severe pleural fibrosis also developed in mice exposed to intrapleural carbon when bleomycin was administered by the intranasal or intraperitoneal route. All together, this suggests that carbon might act as a precipitating or co-factor for bleomycin and thus promote the development of pleural fibrosis. Even more interesting is the observation that this "dual hit" experiment resulted in subpleural fibrosis in the lung parenchyma, very similar to early fibrotic changes in human IPF/UIP.

The detailed mechanisms for this phenomenon are unclear and need to be thoroughly examined. We have previously shown that TGF-β1 overexpression by mesothelial cells can induce subpleural fibrosis together with progressive pleural scarring, suggesting that the mesothelium might be involved in the pathogenesis of pulmonary fibrosis [8]. In these experiments, we provided evidence that matrix accumulation and fibrosis within the subpleural area evolved through a process involving "mesothelial-fibroblastoid transformation" [8]. This is a phenomenon where mesothelial cells acquire myofibroblast characteristics, almost identical to EMT [31]. Mesothelial cells are versatile elements and can exert multiple biological functions [32]. The current study confirms the results from the TGF-β1 overexpression experiments and shows phenotypical changes of mesothelial cells during

the development of bleomycin plus carbon-induced subpleural fibrosis. We found an increase of dual-labelled cytokeratin/ α-SMA-positive cells in the mesothelial layer by day 7 and 21. In contrast, mice exposed to intrapleural bleomycin had these dual-labelled cells only until day 7 and their lungs appeared otherwise normal. These results were supported *in vitro* by demonstrating that mesothelial cells treated with bleomycin acquired myofibroblast characteristics and lost the mesothelial marker E-cadherin. This suggests that bleomycin is able to induce transient "mesothelial-fibroblastoid transformation" in the pleura, but without a second hit (e.g. by carbon particles in our study) this cellular transformation does not persist and does not lead to progressive fibrosis. A recent report by Cool *et al* about the "fibroblastic reticulum" in human IPF, which suggested that fibroblastic foci are organized in a network fashion rather than being isolated areas of cell accumulation, is in general supportive of our hypothesis [33]. However, one would ideally demonstrate mesothelial markers in fibroblast foci from IPF patients to confirm this challenging experimental finding.

The increased levels of TGF-β in the PLF of mice exposed to bleomycin plus carbon indicates that endogenous induction of this profibrotic cytokine might be involved in the progressive fibrotic phenotype. MMP-9 activity was enhanced in the pleural space of these animals, suggesting that the presence of active MMPs may be a critical factor for "mesothelial-fibroblastoid transformation" to be maintained, or to progress and result in "invasive" fibrosis in the pleura and adjacent subpleural areas [8]. There was no correlation between MMP activity and the inflammatory response. Liu *et al.* have demonstrated before that mesothelial cells secrete MMPs in response to phagocytosis of small particles [34], which would explain why MMP-9 is induced in both carbon black and carbon/ bleomycin exposed cells *in vitro* after 48 hours (figure 6B). In the *in vivo* system MMP-9 was only increased in the group that received both carbon black particles and bleomycin (figure 4A). Our hypothesis is that only the concomitant inflammation (caused by co-administration of bleomycin) induces

sustained and mesothelial cell derived MMP-9 activity, and thus facilitates “invasive mesothelial-fibroblastoid transformation”.

In summary, this study shows that intrapleural carbon black is a critical co-factor for the development of bleomycin-induced pleural fibrosis in mice. Experimental pleural fibrosis using this approach is extraordinarily severe and is characterized by major collagen accumulation not only within the pleura but also in the adjacent subpleural area. Mesothelial cells appear to be important contributors to this fibrotic process, possibly through induction of MMPs and TGF-β. These cells have to be considered as targets for further treatment development, both for pleural as well as pulmonary fibrosis.

Table 1

	BALF			
	Total cell count (x10^4)	**Mononucleated cells (%)**	**Lymphocytes (%)**	**Neutrophils (%)**
NaCl	5 +/- 2	99.4 +/- 0.3	0.6 +/- 0.3	0.0 +/- 0.0
CB	9 +/- 3	99.3 +/- 0.2	0.7 +/- 0.2	0.0 +/- 0.0
BL	5 +/- 1	99.0 +/- 0.6	0.6 +/- 0.4	0.4 +/- 0.4
BL+CB	12 +/- 4	98.7 +/- 0.3	0.9 +/- 0.3	0.4 +/- 0.2

	PLF			
	Total cell count (x10^4)	**Mononucleated cells (%)**	**Lymphocytes (%)**	**Neutrophils (%)**
NaCl	8 +/- 2	99.8 +/- 0.2	0.2 +/- 0.2	0.0 +/- 0.0
CB	132 +/- 27	98.6 +/- 0.6	0.6 +/- 0.2	0.8 +/- 0.2
BL	190 +/- 61	97.3 +/- 0.3	0.9 +/- 0.1	1.8 +/- 0.2
BL+CB	144 +/- 39	97.3 +/- 0.4	1.2 +/- 0.2	1.5 +/- 0.4

Table 1: Total and differential cell count in bronchoalveolar lavage fluid (BALF) and pleural lavage fluid (PLF), 7 days after intrapleural injection with NaCl (saline), CB (carbon black), BL (bleomycin) or BL+CB (light grey : $p < 0.03$ vs NaCl ; dark grey : $p < 0.02$ vs NaCl). n = 8 mice for NaCl and CB groups and 12 mice for BL and BL+CB groups.

Table 2

	Day 7	**Day 21**
NaCl	0 +/- 0	0 +/- 0
CB	0 +/- 0	0.3 +/- 0.3
BL	0 +/- 0	0.4 +/- 0.4
BL+CB	1.5 +/- 0.2	3.8 +/- 0.3

Table 2: Pleurodesis scores 7 and 21 days after intrapleural injection with NaCl (saline), CB (carbon black), BL (bleomycin) or BL+CB; 0, normal; 1, < three adhesions; 2, > three adhesions, but localized; 3, generalized scattered adhesions; 4, complete obliteration of the pleural space. BL+CB vs other groups from the same day: $p < 0.001$. n = 8 mice for NaCl and CB groups and 12 mice for BL and BL+CB groups.

Figure Legend

Figure 1:

Carbon Black (CB) did not aggravate bleomycin (BL)-induced pulmonary fibrosis. A) Histology (Masson Trichrome, 100X, scale bar: 100 µm) of mouse lungs 21 days after intratracheal instillation with NaCl, carbon black (CB, 0.1 mg/mouse), BL (0.07 U/mouse) or BL+CB ; B) Histomorphometric quantification of collagen intensity on lung sections, 21 days after intratracheal instillation with NaCl, CB, BL or BL+CB (100 random visual fields per mouse, * $p < 0.0001$ vs. NaCl and CB; no difference between BL and BL+CB). C) Total TGF-β1 in bronchoalveolar lavage fluid 21 days after intratracheal instillation with NaCl, CB, BL or BL+CB (* $p < 0.03$ vs NaCL and CB). n = 8 mice for NaCl and CB groups and 12 mice for BL and BL+CB groups.

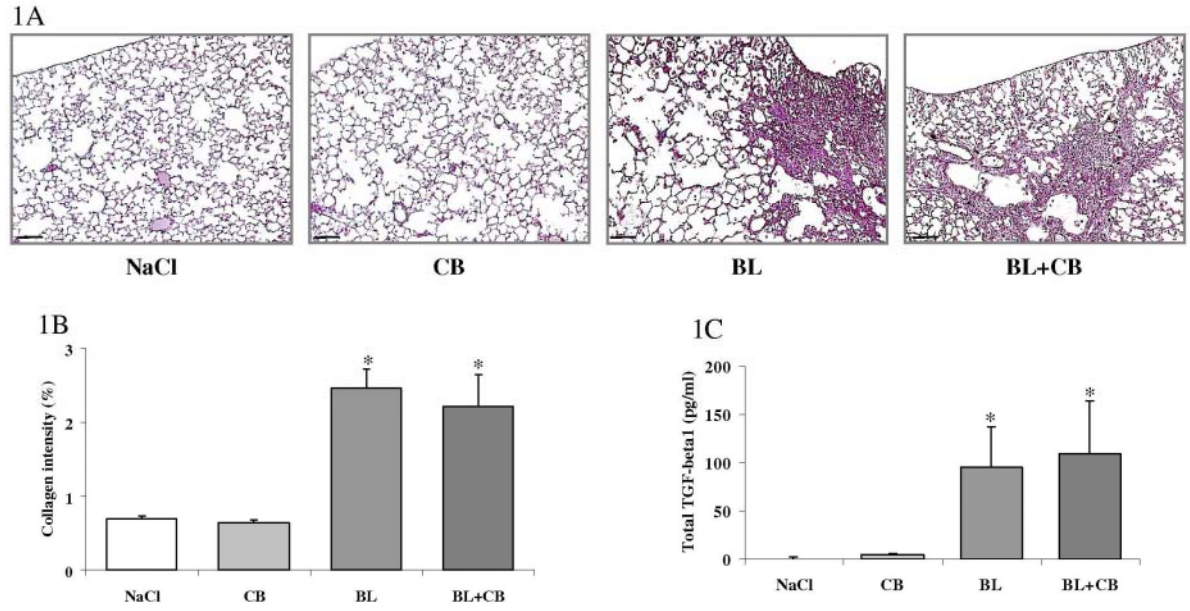

Figure 2:

Intrapleural co-administration of bleomycin (BL) and carbon black (CB) induced severe and progressive pleural and subpleural fibrosis. A) Macroscopic view of the pleura 21 days after intrapleural injection of NaCl, CB (0.1 mg/mouse), BL (0.48 U/mouse) or BL+CB. B) Histology of mouse pleura and subpleural lung parenchyma 21 days after intrapleural injection (Masson Trichrome, 200X, scale bar: 50 µm); C) Histomorphometric quantification of pleural thickness (line) and collagen intensity (bars) on lung sections, 21 days after intrapleural injection with NaCl, CB, BL or BL+CB (20 random visual fields per mouse, * p

< 0.0001 compared with all other groups). D) Histomorphometric quantification of collagen on lung sections in subpleural parenchyma using 2 diameter-constant circles (65 µm) disposed below the pleura, 21 days after intrapleural injection (20 random visual fields per mouse, * p < 0.0001 vs. NaCl and CB, ** p < 0.0001 vs. BL). n = 8 mice for NaCl and CB groups and 12 mice for BL and BL+CB groups.

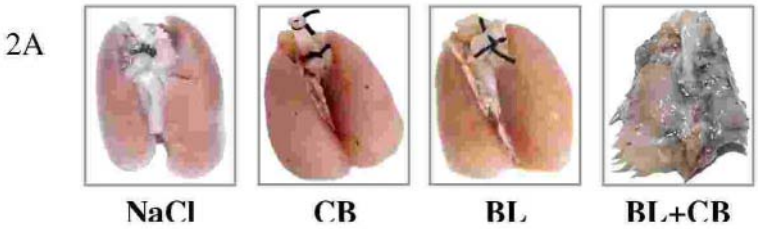
2A
NaCl
CB
BL
BL+CB

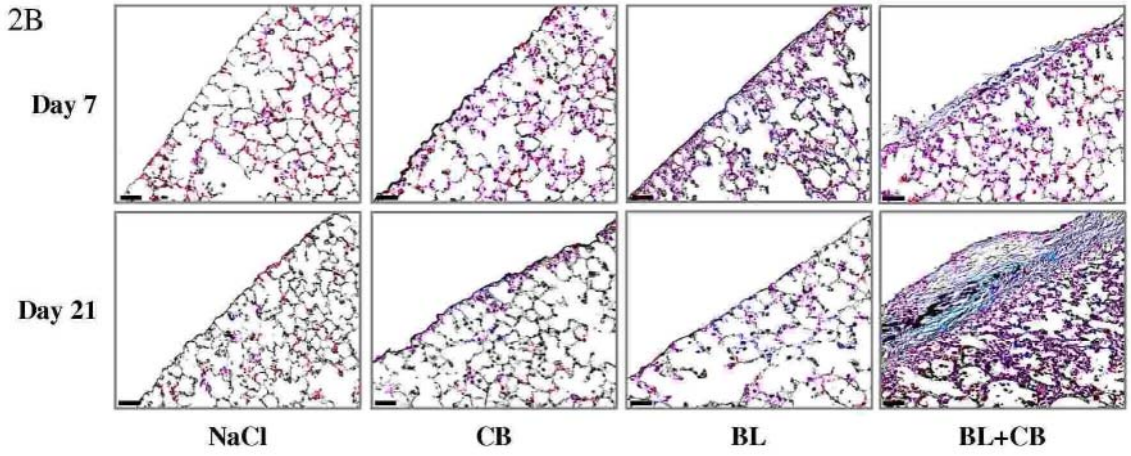
2B
Day 7
Day 21
NaCl
CB
BL
BL+CB

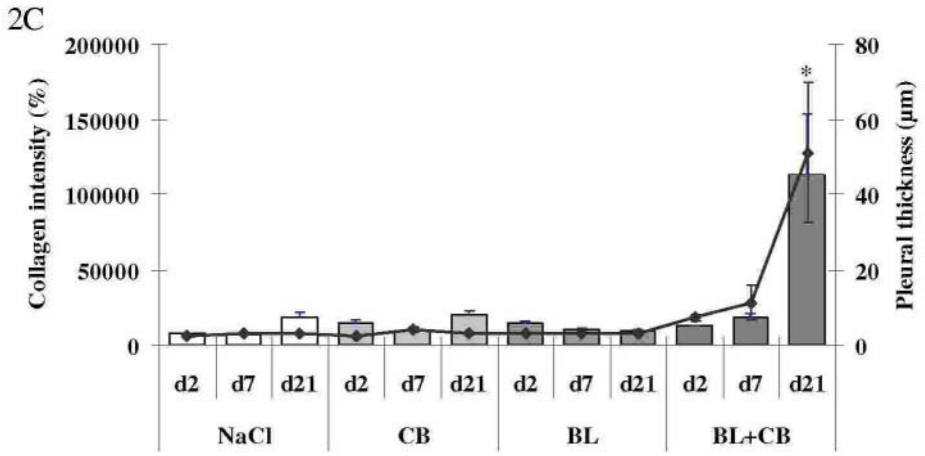
2C
Collagen intensity (%)
Pleural thickness (μm)
200000
150000
100000
50000
0
80
60
40
20
0
*
d2
d7
d21
NaCl
CB
BL
BL+CB

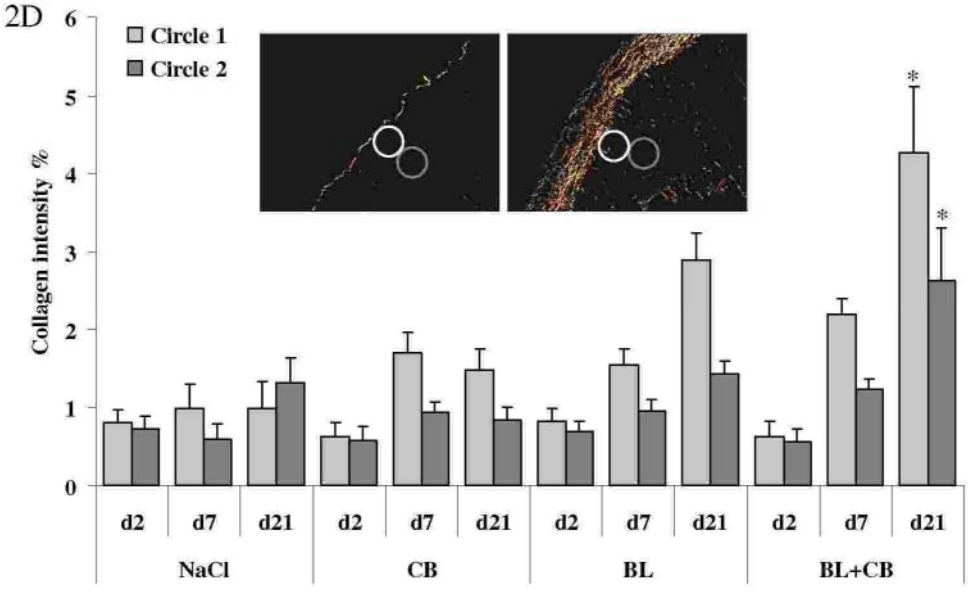
2D
Circle 1
Circle 2
Collagen intensity %
6
5
4
3
2
1
0
*
*
d2
d7
d21
NaCl
CB
BL
BL+CB

Figure 3:

Systemic intraperitoneal (0.48 U/mouse) or intranasal (0.08 U/mouse) bleomycin (BL) combined with intrapleural carbon black (CB) induced pleural fibrosis by day 21 (Masson Trichrome, 100X, scale bar: 100 µm). n = 5 mice for each group.

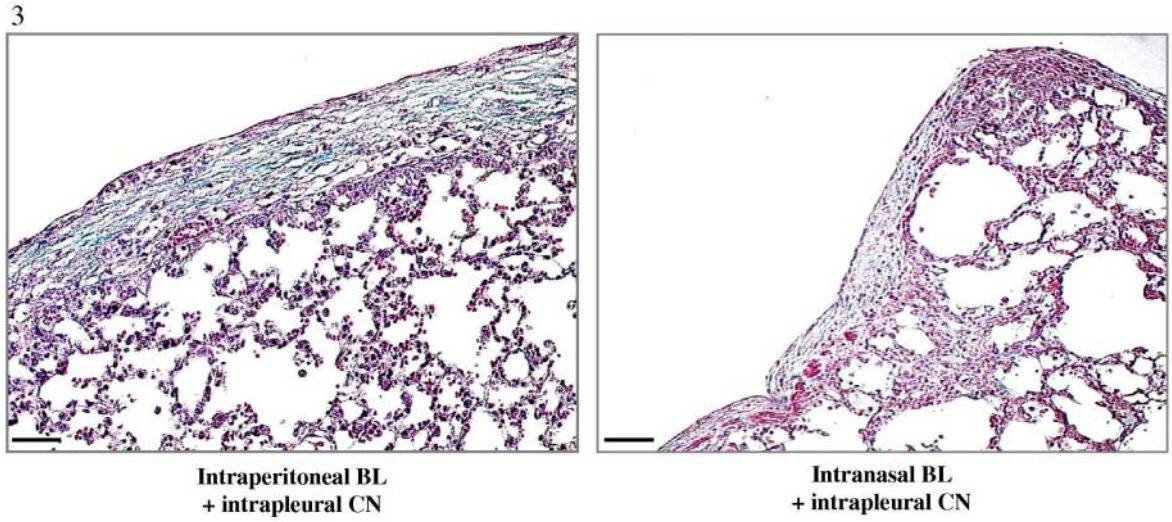

Figure 4:

By immunohistochemistry (500X, scale bar: 20 µm), heat shock protein (HSP)-47 (brown) was slightly overexpressed in mesothelial cells 7 days after carbon black (CB) or bleomycin (BL) intrapleural injection compared to NaCl-treated animals. HSP47 was strongly overexpressed within the pleura and the subpleural area in the BL+CB group. n = 8 mice for NaCl and CB groups and 12 mice for BL and BL+CB groups.

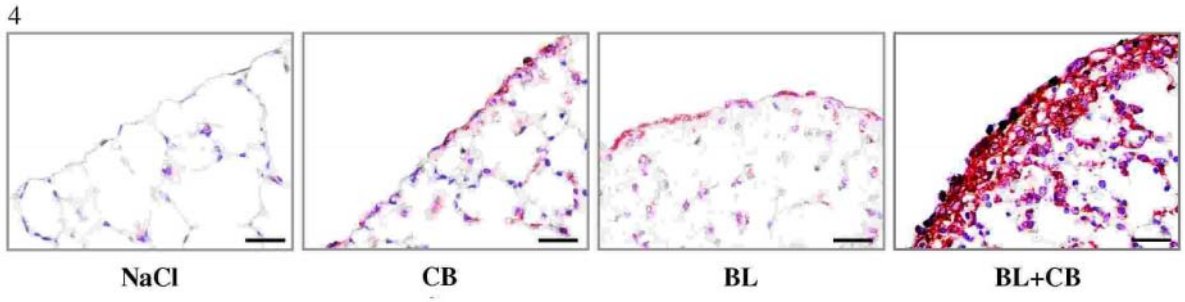

Figure 5:

Mesothelial cells show features of "mesothelial-fibroblastoid transformation", a process similar to epithelial-mesenchymal transition (EMT). A) Gelatin-zymography from pleural lavage fluid (PLF), 7 days after intrapleural injection with NaCl, carbon black (CB),

bleomycin (BL) or BL+CB: matrix metalloproteinase (MMP)-9 activity was only increased in (BL+CB)-treated mice. B) Immunofluorescence on mouse pleura (cytokeratin in green, α-smooth muscle actin (α-SMA) in red, DAPI in blue, 400X, scale bar: 20 µm) showed few dual positive cells in BL-animals and frequent dual-labelled cells in BL+CB-animals (thin arrows) 7 days after intrapleural injection ; these cells were persistent by day 21 and were associated with α-smooth muscle actin (α-SMA)-positive cells (dotted arrow) within the thickened pleura only in BL+CB-animals. C) Total TGF-β1 in pleural lavage fluid (PLF) 7 days after intrapleural injection with NaCl, CB, BL or BL+CB (a: $p < 0.01$ vs NaCl ; b: $p < 0.03$ vs carbon black (CB); c: $p < 0.003$ vs NaCl). n = 8 mice for NaCl and CB groups and 12 mice for BL and BL+CB groups.

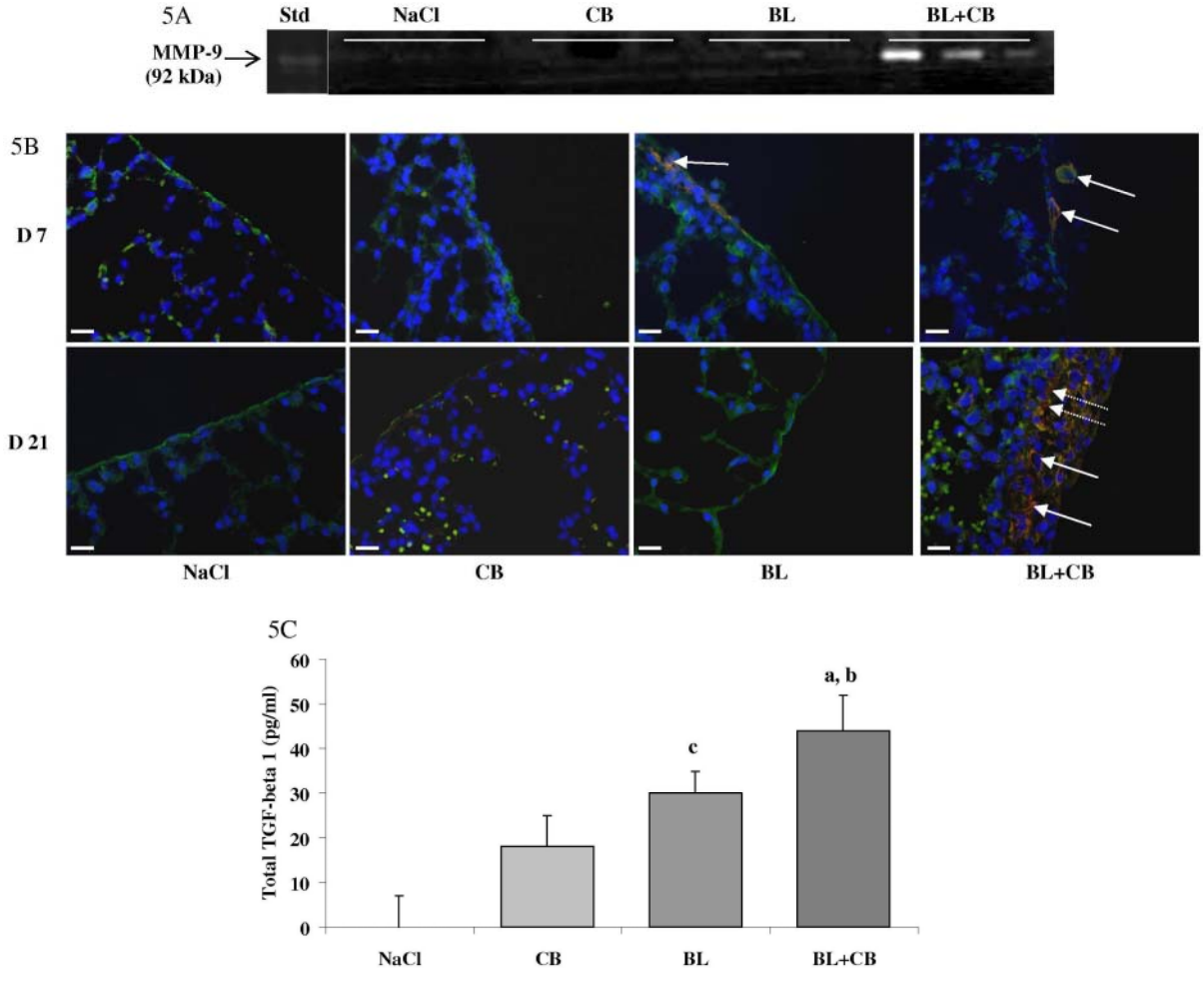

Figure 6:

Mesothelial cell activity in the process of pleural fibrosis. A) ~~Phagocytosis~~ Internalisation of carbon nanoparticles by mesothelial cells (a) i*n vitro* (immunofluorescence, calretinin in green, DAPI in blue, 200X, scale bar: 20 µm) and (b) *in vivo* (lung sections stained by

Masson-Trichrome,21 days after intrapleural injection with carbon black (CB), 500X, scale bar: 20 µm); B) Gelatin-zymography from culture supernatants after mesothelial cell incubation with DMEM, CB (250 µg/ml), bleomycin (BL, 25mU/ml) or BL+CB for 48h: MMP-9 activity was increased after treatment with CB (with or without BL). This experiment was repeated three times. C) Immunofluorescence on 4/4RM4 mesothelial cells with α-SMA (green, top line), E-cadherin (green, bottom line), DAPI in blue, 630X, scale bar : 10 µm) showed an increase in α-SMA and a decrease in E-cadherin after 48h-treatment with bleomycin or bleomycin + carbon.

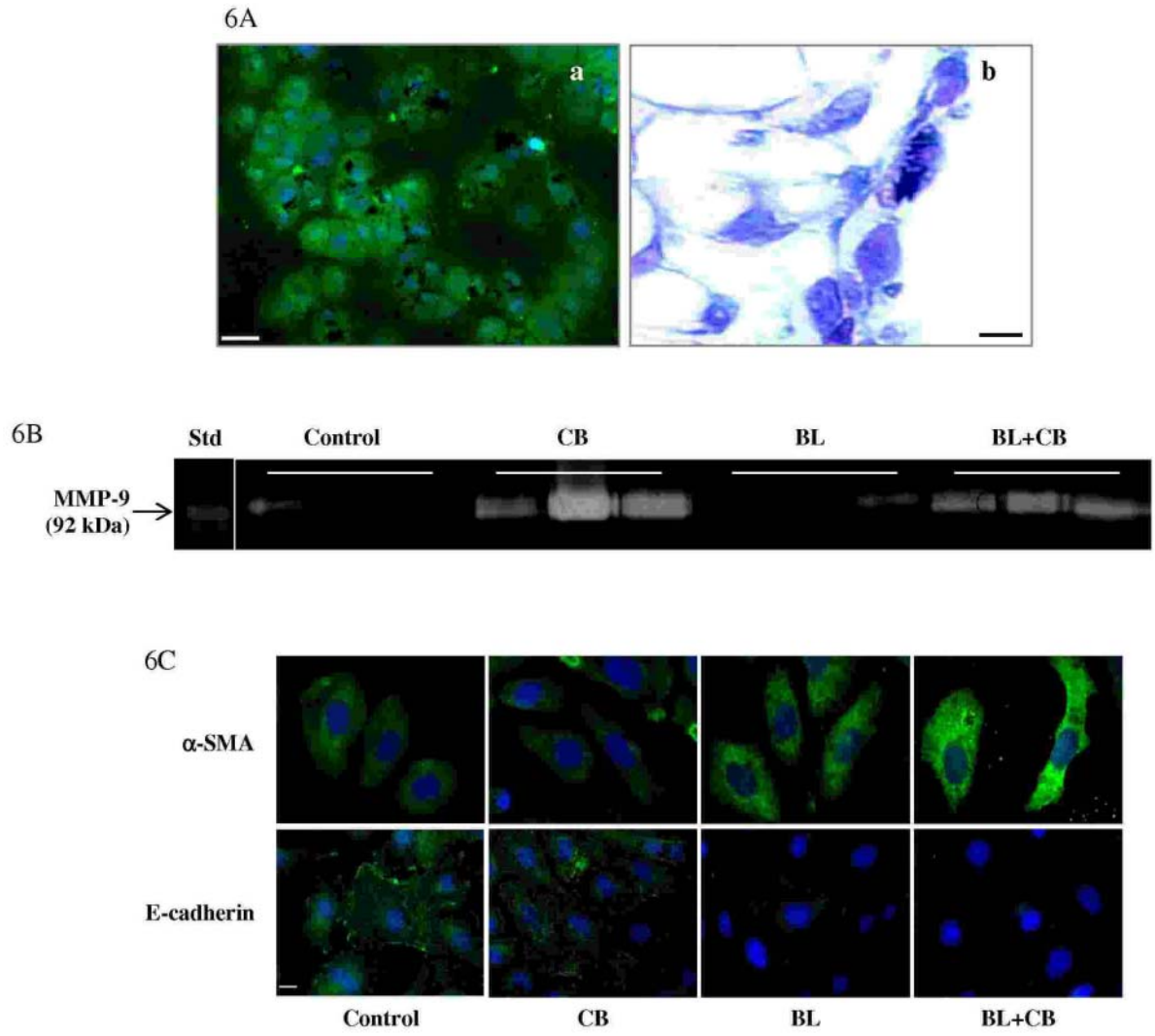

Acknowledgments

The authors thank V. San Giorgio and all the team from the animal quarter for their invaluable and professional help.

Conflict of interest

The authors declare no conflict of interest or financial interests.

References

1. Jantz MA, Antony VB. Pleural fibrosis. *Clin Chest Med* 2006: 27(2): 181-191.
2. Azoulay E, Paugam B, Heymann MF, Kambouchner M, Haloun A, Valeyre D, Battesti JP, Tazi A. Familial extensive idiopathic bilateral pleural fibrosis. *Eur Respir J* 1999: 14(4): 971-973.
3. Becker CD, Gil J, Padilla ML. Idiopathic pleuroparenchymal fibroelastosis: an unrecognized or misdiagnosed entity? *Mod Pathol* 2008.
4. Frankel SK, Cool CD, Lynch DA, Brown KK. Idiopathic pleuroparenchymal fibroelastosis: description of a novel clinicopathologic entity. *Chest* 2004: 126(6): 2007-2013.
5. Lee YC, Light RW. Management of malignant pleural effusions. *Respirology* 2004: 9(2): 148-156.
6. Light RW. Talc for pleurodesis? *Chest* 2002: 122(5): 1506-1508.
7. Geiser T. Idiopathic pulmonary fibrosis--a disorder of alveolar wound repair? *Swiss Med Wkly* 2003: 133(29-30): 405-411.
8. Decologne N, Kolb M, Margetts PJ, Menetrier F, Artur Y, Garrido C, Gauldie J, Camus P, Bonniaud P. TGF-beta1 induces progressive pleural scarring and subpleural fibrosis. *J Immunol* 2007: 179(9): 6043-6051.
9. Cooper JA, Jr., White DA, Matthay RA. Drug-induced pulmonary disease. Part 1: Cytotoxic drugs. *Am Rev Respir Dis* 1986: 133(2): 321-340.
10. www.pneumotox.com. The drug-induced lung diseases. [Website] 2002 July, 2002 [cited 1996; Available from:
11. Antony VB, Loddenkemper R, Astoul P, Boutin C, Goldstraw P, Hott J, Rodriguez Panadero F, Sahn SA. Management of malignant pleural effusions. *Eur Respir J* 2001: 18(2): 402-419.
12. Baumgartner KB, Samet JM, Stidley CA, Colby TV, Waldron JA. Cigarette smoking: a risk factor for idiopathic pulmonary fibrosis. *Am J Respir Crit Care Med* 1997: 155(1): 242-248.
13. Lower EE, Strohofer S, Baughman RP. Bleomycin causes alveolar macrophages from cigarette smokers to release hydrogen peroxide. *The American journal of the medical sciences* 1988: 295(3): 193-197.
14. Cisneros-Lira J, Gaxiola M, Ramos C, Selman M, Pardo A. Cigarette smoke exposure potentiates bleomycin-induced lung fibrosis in guinea pigs. *American journal of physiology* 2003: 285(4): L949-956.
15. Valente P, Forastiere F, Bacosi A, Cattani G, Di Carlo S, Ferri M, Figa-Talamanca I, Marconi A, Paoletti L, Perucci C, Zuccaro P. Exposure to fine and ultrafine particles from secondhand smoke in public places before and after the smoking ban, Italy 2005. *Tob Control* 2007: 16(5): 312-317.
16. Holt PF. Translocation of inhaled dust to the pleura. *Environ Res* 1983: 31(1): 212-220.
17. Marchi E, Vargas FS, Acencio MM, Teixeira LR, Antonangelo L, Lee YC, Light RW. Pleurodesis: a novel experimental model. *Respirology* 2007: 12(4): 500-504.
18. Kakugawa T, Mukae H, Hayashi T, Ishii H, Abe K, Fujii T, Oku H, Miyazaki M, Kadota J, Kohno S. Pirfenidone attenuates expression of HSP47 in murine bleomycin-induced pulmonary fibrosis. *Eur Respir J* 2004: 24(1): 57-65.
19. American Thoracic Society. Idiopathic pulmonary fibrosis: diagnosis and treatment. International consensus statement. American Thoracic Society (ATS), and the European Respiratory Society (ERS). *Am J Respir Crit Care Med* 2000: 161(2 Pt 1): 646-664.

20. Moeller A, Ask K, Warburton D, Gauldie J, Kolb M. The bleomycin animal model: a useful tool to investigate treatment options for idiopathic pulmonary fibrosis? *The international journal of biochemistry & cell biology* 2008: 40(3): 362-382.
21. Borzone G, Moreno R, Urrea R, Meneses M, Oyarzun M, Lisboa C. Bleomycin-induced chronic lung damage does not resemble human idiopathic pulmonary fibrosis. *Am J Respir Crit Care Med* 2001: 163(7): 1648-1653.
22. Jones AW, Reeve NL. Ultrastructural study of bleomycin-induced pulmonary changes in mice. *The Journal of pathology* 1978: 124(4): 227-233.
23. Lee YC, Baumann MH, Maskell NA, Waterer GW, Eaton TE, Davies RJ, Heffner JE, Light RW. Pleurodesis practice for malignant pleural effusions in five English-speaking countries: survey of pulmonologists. *Chest* 2003: 124(6): 2229-2238.
24. Lee YC, Lane KB, Parker RE, Ayo DS, Rogers JT, Diters RW, Thompson PJ, Light RW. Transforming growth factor beta(2) (TGF beta(2)) produces effective pleurodesis in sheep with no systemic complications. *Thorax* 2000: 55(12): 1058-1062.
25. Sekhon H, Wright J, Churg A. Effects of cigarette smoke and asbestos on airway, vascular and mesothelial cell proliferation. *International journal of experimental pathology* 1995: 76(6): 411-418.
26. Donaldson K, Aitken R, Tran L, Stone V, Duffin R, Forrest G, Alexander A. Carbon nanotubes: a review of their properties in relation to pulmonary toxicology and workplace safety. *Toxicol Sci* 2006: 92(1): 5-22.
27. Andre E, Stoeger T, Takenaka S, Bahnweg M, Ritter B, Karg E, Lentner B, Reinhard C, Schulz H, Wjst M. Inhalation of ultrafine carbon particles triggers biphasic pro-inflammatory response in the mouse lung. *Eur Respir J* 2006: 28(2): 275-285.
28. Donaldson K, Stone V, Tran CL, Kreyling W, Borm PJ. Nanotoxicology. *Occup Environ Med* 2004: 61(9): 727-728.
29. Beattie J, Knox JF. Studies of mineral content and particle size distribution in the lungs of asbestos textile workers. *In "Inhaled Particles and Vapours" (CN Davis, Ed)* 1961: 419-432.
30. Adamson IY, Prieditis HL. Response of mouse lung to carbon deposition during injury and repair. *Environ Health Perspect* 1995: 103(1): 72-76.
31. Willis BC, Borok Z. TGF-beta-induced EMT: mechanisms and implications for fibrotic lung disease. *American journal of physiology* 2007: 293(3): L525-534.
32. Mutsaers SE. Mesothelial cells: their structure, function and role in serosal repair. *Respirology* 2002: 7(3): 171-191.
33. Cool CD, Groshong SD, Rai PR, Henson PM, Stewart JS, Brown KK. Fibroblast foci are not discrete sites of lung injury or repair: the fibroblast reticulum. *Am J Respir Crit Care Med* 2006: 174(6): 654-8
34. Liu W, Ernst JD, Broaddus VC. Phagocytosis of crocidolite asbestos induces oxidative stress, DNA damage, and apoptosis in mesothelial cells. *Am J Respir Cell Mol Biol* 2000: 23(3): 371-378.